

## Recent advances in dynamical modeling and attitude control of flexible spacecraft

David Paolo Madonna<sup>1,a\*</sup>

<sup>1</sup>Department of Mechanical and Aerospace Engineering, Sapienza University of Rome, Via Eudossiana 18, 00184 Rome, Italy

<sup>a</sup>davidpaolo.madonna@uniroma1.it

**Keywords:** Flexible Spacecraft, Stress Stiffening, Kane's Method, Nonlinear Feedback Attitude Control, Control Momentum Gyroscopes

**Abstract.** This work is focused on some recent advances on spacecraft dynamical modeling and attitude control. First, the problem of correctly linearizing the elastic behavior of spinning flexible spacecraft is discussed, and an example is presented that addresses this topic from both the analytical and the numerical point of view. Then, attitude control is considered and a new feedback law for single axis alignment is presented, together with the inclusion of accurate modeling of the actuation dynamics. Moreover, numerical simulations for the reorientation of a flexible multibody spacecraft are provided.

### Introduction

Current space missions require predicting the spacecraft dynamics with considerable reliability. Among the various components of a spacecraft, subsystems like payload, structures, and power depend heavily on the dynamic behavior of the satellite during its operational life. Therefore, to ensure that the results obtained through numerical simulations correspond to the actual behavior, an accurate dynamical model must be developed. Reducing the margins of uncertainty implies the possibility of carrying out proper sizing of various features of the system, while on the other side it allows enhancing the mission performance.

Although in several cases it is acceptable to model the spacecraft as a single rigid body, in specific applications the satellite must be modeled as a multibody system composed of both rigid and flexible elements, to get higher accuracy. This occurs because the dynamic behavior of a spacecraft can be affected by many factors, including structural deformations, vibrations, and disturbances that arise from its interaction with the space environment.

In this perspective, when dealing with flexible spacecraft that undergo a high-speed rotation, it may become necessary to include the stress stiffening in the model, which is the increase in stiffness due to internal stresses produced by the inertial loads [1]. This phenomenon is included in the dynamical model only if the nonlinear elastic behavior of the flexible bodies is considered. In Section II, the procedure to correctly linearize the dynamical equations of a flexible spacecraft to preserve the stress stiffening effect is discussed and the error produced by a premature linearization is investigated.

Once a detailed model has been obtained, a suitable control architecture must be designed and tested on the complete model to ensure proper control of the spacecraft for both orbit and attitude control. In Section III, nonlinear feedback control strategies are investigated, which have the advantage of ensuring convergence for large-angle maneuvers even in attitude tracking scenarios [2]. In addition to control strategies, actuation is also studied, with a focus on momentum exchange devices, specifically single-gimbal control momentum gyroscopes. Suitable steering laws are analyzed to achieve accurate tracking and prevent singularities [3].



### Stress stiffening

The stress stiffening phenomenon, commonly observed in high-speed flexible rotating satellites, has a significant impact on the dynamical behavior and stability of the spacecraft [4]. Specifically, a flexible spacecraft subject to fast rotational motion shows a dynamic stiffening effect induced by the stresses generated by the inertia loads. However, this is frequently overlooked in dynamical modeling when attitude control is designed, and the dynamic equations are linearized around the equilibrium position of the satellite. Of course, neglecting this phenomenon in case of spinning satellites can lead to a wrong representation of the real behavior of the structure and consequently errors in the elastic displacements as shown in some examples reported in Ref [5].

Kane’s formulation of multibody spacecraft dynamics introduces partial velocities, to relate the Newton/Euler dynamical quantities to generalized velocities [6]. In this framework, stress stiffening is taken into account by linearizing the dynamical equations after the extraction of partial velocities. Unfortunately, this procedure is not easy to implement for complex spacecraft where the flexible elements can be described from the static and dynamic point of view using discrete formulations such as Finite Element Modeling (FEM). To overcome this challenge, it is recommended to first perform a linear static analysis of the flexible elements using FEM to determine the stress configuration under given inertial loading conditions. Then, this stress configuration can be used to compute the increment in strain energy due to nonlinear elastic deformations, to obtain a “stress stiffening matrix”, which can be added a posteriori to the linear stiffness, with the final aim of deriving the complete equations of motion for the flexible elements [7].

A preliminary analysis is conducted to evaluate the effectiveness of the procedure described above, using a rotating cantilever beam as a case study (see Fig.1). The beam is assumed to undergo planar motion, while flexibility is modeled using a single elastic bending mode. This simple example allows for a clear identification of the contribution of stress stiffening in the dynamical equations.

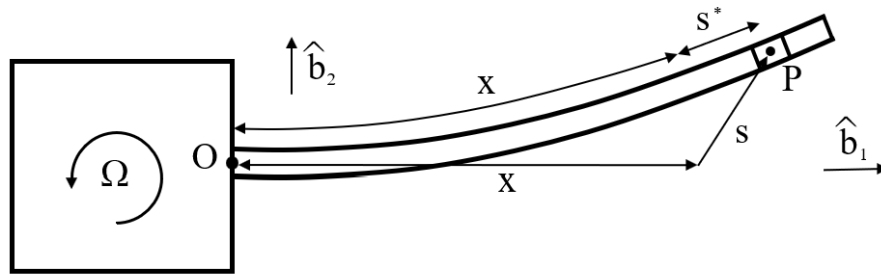


Figure 1: sketch of a rotating cantilever beam

Similarly to the more general case, in this example nonlinear velocities are obtained by including the nonlinear elastic behavior of the structure in the analysis. Referring to Fig. 1, if  $x$  is the distance  $OP$  when the beam is undeformed and neglecting the axial elastic displacement (as it has been assumed in this analysis), i.e. letting  $s^* = 0$ , one can write that

$$x = \int_0^\xi \sqrt{1 + \left( \frac{\partial s_2(\sigma, t)}{\partial \sigma} \right)^2} d\sigma \quad (1)$$

where  $\mathbf{s} = [s_1 \quad s_2 \quad 0]^T$  is the elastic displacement,  $\xi = x + s_1$  and  $\sigma$  is a dummy variable.  $J$  is introduced as

$$J(\sigma, t) \equiv 1 + \left( \frac{\partial s_2(\sigma, t)}{\partial \sigma} \right)^2. \tag{2}$$

The bending elastic displacement is decomposed through the well-established modal decomposition approach [8] as

$$s_2(x, t) = \sum_{i=1}^v \varphi_{2i}(x) q_i(t), \tag{3}$$

where  $v$  denotes the number of flexible degrees of freedom of the beam,  $q_i(t)$  is the  $i$ -th modal amplitude and  $\varphi_{2i}(x)$  is the  $i$ -th eigenfunction associated with the bending motion. The following time derivative is obtained from Eq. 1:

$$\dot{s}_1 = \frac{1}{\sqrt{J(\xi, t)}} \sum_{i=1}^v \left\{ -\sum_{j=1}^v q_j(t) \int_0^\xi \frac{1}{\sqrt{J(\sigma, t)}} \left( \frac{\partial \varphi_{2i}(\sigma)}{\partial \sigma} \right)^2 d\sigma \right\} q_i(t). \tag{4}$$

Hence, although axial elasticity is not included in the model by assumption, the component of the elastic displacement along  $\hat{\mathbf{b}}_1$  is nonzero because of the correlation with the bending displacement, which would not have appeared in the equations if only linear strain-displacement relations had been considered. Using Eq. 4, the following nonlinear velocities are obtained:

$$\mathbf{v}_p = \tilde{\boldsymbol{\Omega}} \mathbf{r}_{op} + \dot{\mathbf{s}} \tag{5}$$

where  $\mathbf{C} = [0 \quad 0 \quad \boldsymbol{\Omega}]^T$  and  $\mathbf{r}_{op}$  is the distance from  $O$  to  $P$  in the deformed configurations. It is possible to extract nonlinear partial velocities, which now can be correctly linearized with respect to small elastic displacements assuming the following form:

$$\mathbf{V} = \begin{bmatrix} -\beta_{11}(x) q_1(t) \\ \varphi_{21} \\ 0 \end{bmatrix} \tag{6}$$

where

$$\beta_{11}(x) = \int_0^x \left( \frac{\partial \varphi_{21}(\sigma)}{\partial \sigma} \right)^2 d\sigma. \tag{7}$$

Instead, extracting the partial velocities from linearized expressions of the velocity (i.e. Eq. 5 with  $\dot{s}_1 = 0$ ) implies obtaining the following incomplete vector:

$$\bar{\mathbf{V}} = \begin{bmatrix} 0 \\ \varphi_{21} \\ 0 \end{bmatrix}, \tag{8}$$

which leads to a lack of terms in the dynamical equations. Once the correct partial velocities have been extracted, the linearized velocity can be derived to obtain the acceleration of the points of the beam

$$\mathbf{a}_p = \bar{\mathbf{V}}\ddot{\mathbf{q}}(t) + \mathbf{a}_p^{(R)} \tag{9}$$

where  $\mathbf{a}_p^{(R)}$  collects the terms of  $\mathbf{a}_p$  that do not depend on the time derivatives of generalized velocities. Hence, the following form of Kane’s dynamical equations is used [9]:

$$\int_0^L \rho(x) \mathbf{V}^T \bar{\mathbf{V}} dx \ddot{\mathbf{q}}(t) + \int_0^L \rho(x) \mathbf{V}^T \mathbf{a}_p^{(R)} dx + \omega_b^2 \mathbf{q}(t) = 0, \tag{10}$$

where  $L$  is the beam length,  $\rho(x)$  is the beam mass per unit of length and  $\omega_b$  is the frequency of the bending mode. Then, one obtains the final governing equation,

$$\ddot{\mathbf{q}}(t) + \{\omega_b^2 - \Omega^2 + \lambda\Omega^2\} \mathbf{q}(t) = -\dot{\Omega} \int_0^L \rho(x) x \varphi_{21}(x) dx. \tag{11}$$

The term

$$\lambda = \int_0^L \rho(x) \beta_{11}(x) x dx > 1 \tag{12}$$

is responsible for the stress stiffening. It is worth noting that coupling between the rigid rotation and the elastic displacement of the beam, here represented by the amplitude of the modal shape  $q(t)$ , has two opposite effects. The first effect, associated with the linearized flexible dynamics and represented by the term  $\{\omega_b^2 - \Omega^2\} q(t)$  is responsible of the “reduction” of the internal stiffness of the beam. The second effect, corresponding to  $\{\lambda\Omega^2\} q(t)$  is related to the centrifugal action that stretches and stiffens the beam. It is important to observe that if  $\Omega^2 = \omega_b^2$  the “effective stiffness” of the beam would vanish if the centrifugal term were omitted leading to a completely misrepresentation of the real dynamic behavior of the rotating beam.

**Table 1: beam's physical properties**

Density ( $\rho$ )	1.2 [kg / m]
Length ( $L$ )	10 [m]
Young’s modulus ( $E$ )	$7 \cdot 10^{10}$ [N / m <sup>2</sup> ]
Area moment of inertia ( $I$ )	$2 \cdot 10^{-7}$ [m <sup>4</sup> ]
First bending frequency ( $\omega_b$ )	0.6044 [Hz]

In this study, numerical simulations are conducted based on the data presented in Table 1, to investigate the elastic behavior of a cantilever beam subject to a rotation motion following a cubic law. The maximum tip displacements (with and without stiffening effects) are plotted against the ratio of the beam angular velocity to its first bending natural frequency, as shown in Fig. 2. As stated above the results indicate that linearizing the partial velocities prematurely leads to a significant increase in error even when  $\Omega / \omega_b < 1$ . In Fig. 3 the time histories of tip displacement for  $\Omega = 6 \text{ rad/s}$  are reported.

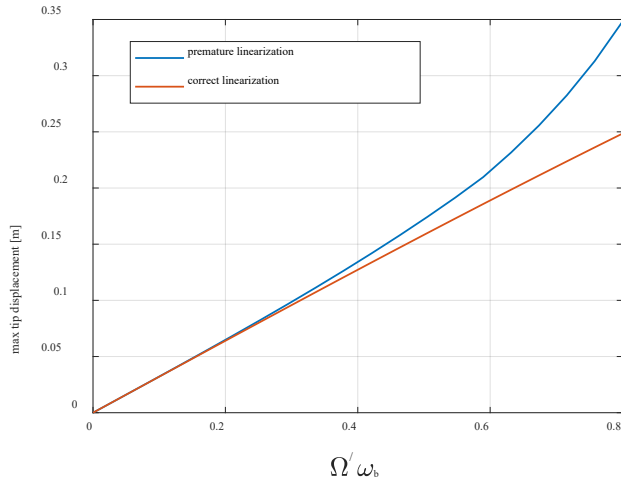


Figure 2: max tip displacement vs angular velocity

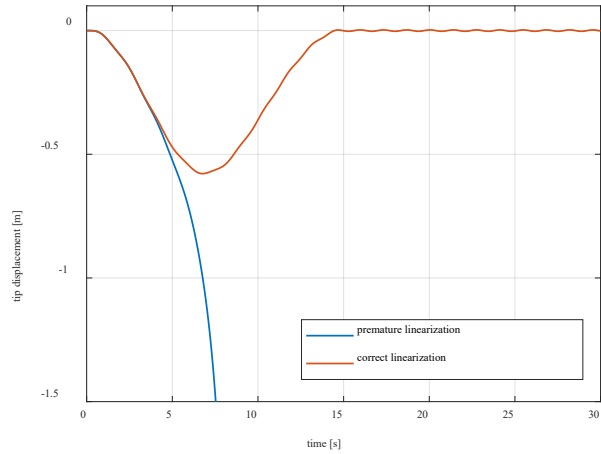


Figure 3: tip displacement for  $\Omega = 6 \text{ rad/s}$

With a premature linearization one obtains wrong results, while the beam shows a completely different behavior. Hence, considering the stress stiffening effects allows reducing the margin of safety while designing space systems that undergo fast motion conditions.

### Nonlinear attitude control applied to spacecraft dynamics.

It is well known that accurate dynamical modeling of multibody spacecraft is essential in designing their attitude control system. The motion of the spacecraft components, including robotic arms and steerable solar panels, as well as elastic oscillations of the structures, profoundly impact the attitude dynamics. Therefore, these factors must be considered during the synthesis of the attitude control, which is the topic addressed in this section.

In the following, a significant attention is paid on nonlinear feedback control laws, which ensure convergence in terms of attitude and angular velocity for large-angle maneuvers even when tracking is required [10]. In particular, the triaxial feedback control torque can be represented in its nonlinear form as

$$\mathbf{T}_C = \tilde{\boldsymbol{\omega}} \mathbf{J}_C \boldsymbol{\omega} - \mathbf{M}_C + \mathbf{J}_C \dot{\boldsymbol{\omega}}_C - \mathbf{J}_C \mathbf{A}^{-1} \mathbf{B} \boldsymbol{\omega}_D - \text{sgn}\{\mathbf{q}_{e_0}(t_0)\} \mathbf{J}_C \mathbf{A}^{-1} \mathbf{q}_e, \quad (13)$$

where  $\boldsymbol{\omega}$  is the angular velocity of the spacecraft,  $\mathbf{J}_C$  is the moment of inertia computed with respect of the center of mass,  $\mathbf{M}_C$  is the vector of known disturbance torques,  $\boldsymbol{\omega}_C$  is the commanded angular velocity vector,  $\boldsymbol{\omega}_D = \boldsymbol{\omega} - \boldsymbol{\omega}_C$  is the simplified error angular velocity,  $\{\mathbf{q}_{e_0}, \mathbf{q}_e\}$  is the error quaternion associated with the misalignment between the commanded frame and the body frame and  $\mathbf{A}$  and  $\mathbf{B}$  are gain matrices that must be positive definite ( $\mathbf{A}$  must also be

symmetric); finally, the sign of  $q_{e_0}(t_0)$  is introduced to choose the shortest path to reach the desired attitude.

When it is sufficient to drive only a single axis toward a desired direction, a reduced-attitude control law can be applied to further improve the results, as shown in Refs. [9,11]. A new reduced-attitude control law is derived and presented by the author in Ref. [12]. The expression of this control law is the following:

$$\mathbf{T}_C = \tilde{\boldsymbol{\omega}} \mathbf{J}_C \boldsymbol{\omega} - \mathbf{M}_C + \mathbf{J}_C \left[ \mathbf{R}_{B \leftarrow C} \dot{\boldsymbol{\omega}}_C - \tilde{\boldsymbol{\omega}}_e \mathbf{R}_{B \leftarrow C} \boldsymbol{\omega}_C \right] - \mathbf{J}_C \mathbf{A}^{-1} \mathbf{B} \boldsymbol{\omega}_e - \mathbf{J}_C \mathbf{A}^{-1} \mathbf{g}(q_{e_0}^M, \mathbf{q}_e^M) \quad (14)$$

$$\mathbf{g}(q_{e_0}^M, \mathbf{q}_e^M) = 2 \begin{bmatrix} 0 \\ q_{e_0}^M q_{e_2}^M + q_{e_1}^M q_{e_3}^M \\ q_{e_0}^M q_{e_3}^M - q_{e_1}^M q_{e_2}^M \end{bmatrix} \quad (15)$$

where  $\mathbf{R}_{B \leftarrow C}$  is the rotation matrix from the commanded frame to the body frame,  $\boldsymbol{\omega}_e = \boldsymbol{\omega} - \mathbf{R}_{B \leftarrow C} \boldsymbol{\omega}_C$  is the error angular velocity and  $\{q_{e_0}^M, \mathbf{q}_e^M\}$  is a modified error quaternion. In the case it is required to drive the body axis  $\hat{b}_1$  toward the commanded axis  $\hat{b}_{C,1}$ , the modified error quaternion is associated with the misalignment between the commanded frame and a frame obtained from the body frame through an eigenaxis rotation, for which

- the eigenangle  $\phi$  is defined as  $\phi = \cos^{-1}(\hat{b}_1 \cdot \hat{b}_{C,1})/2$ , and
- the eigenaxis corresponds to  $\hat{e} = \frac{\hat{b}_1 \times \hat{b}_{C,1}}{\|\hat{b}_1 \times \hat{b}_{C,1}\|}$ .

The global asymptotic stability of the control law reported in Eqs. 16-17 is proven by the author in Ref. [12].

Moreover, the actuators' dynamics of the momentum exchange devices are also considered by the author in [9,12], to implement a high-fidelity control law. In particular, single gimbal control momentum gyroscopes (SG-CMGs) are used because they can provide the desired torque requiring a reduced amount of power compared to other actuators. However, their main drawback is that they suffer from specific singular configurations, which prevent from providing the desired torque to the spacecraft.

In Refs. [9,12], accurate steering laws are used to reduce the error in the control torque introduced by the actuator dynamics. In particular, further terms that take the detailed model of the actuators into account are added to the steering law commonly used in the literature [3], to significantly improve the accuracy of the actuators' torque. Furthermore, singularity avoidance algorithms are studied and applied to this enhanced steering law to escape from singular configurations. Specifically, a small error in the commanded torque is introduced to make the gyros move away from singularity. The magnitude of this error is opportunely reduced through a singularity direction avoidance (SDA) pseudoinverse law. Moreover, sizing of the pyramidal arrays of SG-CMGs is also investigated, to guarantee storage of angular momentum in any direction so that the desired angular velocities can be approached and achieved [13].

A Monte Carlo campaign is carried out to simulate attitude maneuvers for a large flexible spacecraft that mounts a pyramidal array of SG-CMGs, steered using the techniques described before. In particular, the performance of the new reduced-attitude control law is compared the one obtained using triaxial control law of Eq. 15, and results are reported in Figs. 4 and 5.

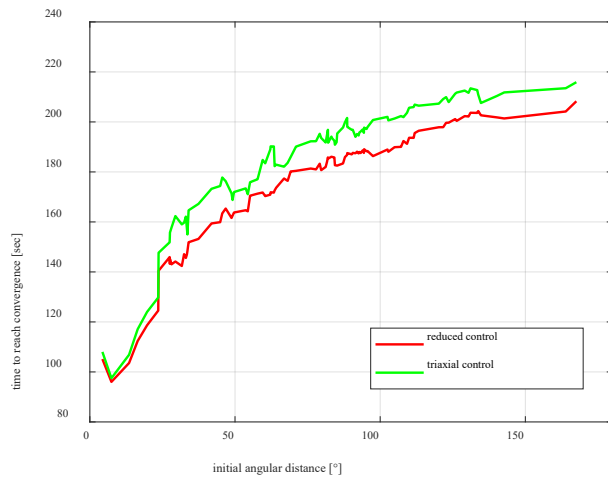


*Figure 4: convergence time vs initial angular distance*

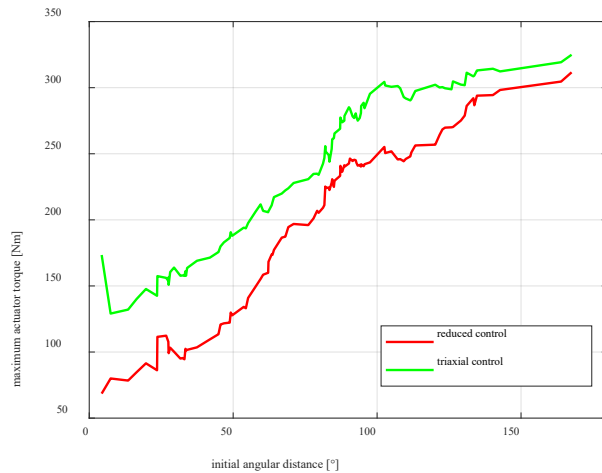


*Figure 5: max torque vs initial angular distance*

From inspection of Figs. 4-5, it is apparent that the reduced-attitude control law is always preferable (assuming that single-axis control is required) because it ensures faster convergence while requiring lower torques.

### Conclusions

In the first part, a discussion about the correct linearization of dynamical equations of a rotating flexible body highlights how stress stiffening affects the equations of motion, and the effect of neglecting this phenomenon is numerically evaluated. Then, techniques to design the attitude control system are discussed, also dealing with sizing and steering of arrays of single gimbal control momentum gyroscopes. The performance of a new nonlinear feedback control law is compared to that of an existing law, to point out its advantages in terms of convergence time and torque requirement.

### References

- [1] T. R. Kane, R. Ryan, A. K. Banerjee, Dynamics of a Cantilever Beam Attached to a Moving Base, *Journal of Guidance, Control, and Dynamics*, Volume 10, Issue 2, 1987. <https://doi.org/10.2514/3.20195>
- [2] A. H. de Ruiter, C. Damaren, J. Forbes, *Spacecraft Dynamics and Control: An Introduction*, Wiley, 2013. <https://doi.org/10.5860/choice.51-0301>
- [3] F. A. Leve, B. Hamilton, M. Peck, *Spacecraft Momentum Control Systems*, Springer, 2015. <https://doi.org/10.1007/978-3-319-22563-0>
- [4] P. Santini, Stability of flexible spacecrafts, *Acta Astronautica*, Volume 3, Issues 9–10, Pages 685-713, 1976. [https://doi.org/10.1016/0094-5765\(76\)90106-5](https://doi.org/10.1016/0094-5765(76)90106-5)
- [5] A. K. Banerjee, *Flexible Multibody Dynamics: Efficient Formulations and Applications*, Wiley, 2016. <https://doi.org/10.1002/9781119015635>
- [6] T. R. Kane, P. W. Likins, D. A. Levinson, *Spacecraft Dynamics*, McGraw-Hill, 1983.

- [7] R. D, Cook, Concepts and Applications of Finite Element Analysis, McGraw-Hill, 1985.
- [8] S. Rao, Vibration of Continuous Systems, Wiley, 2007.  
<https://doi.org/10.1002/9780470117866>
- [9] D. P. Madonna, M. Pontani, P. Gasbarri, Attitude Maneuvers of a Flexible Spacecraft for Space Debris Detection and Collision Avoidance, Proceedings of the 73<sup>rd</sup> International Astronautical Congress, Paper IAC-22,C1,2,1,x68387, 2022.
- [10] M. Pontani, Booklets and lecture notes of Space and Astronautical Engineering course “Advanced Spacecraft Dynamics”
- [11] M. Pontani, I. Napoli, A New Guidance and Control Architecture for Orbit Docking via Feedback Linearization, Proceedings of the 73<sup>rd</sup> International Astronautical Congress, Paper IAC-21-C1.1.14, 2021.
- [12] D. P. Madonna, M. Pontani, P. Gasbarri, Nonlinear Attitude Maneuvering of a Flexible Spacecraft for Space Debris Tracking and Collision Avoidance, submitted to Acta Astroanutica.
- [13] A. Mony, H. Hablani, G. Sharma, Control Momentum Gyro (CMG) Sizing and Cluster Configuration Selection for Agile Spacecraft 10th National Symposium and Exhibition on Aerospace and Related Mechanisms, 2016.